

# Square-Extensional Mode Single-Crystal Silicon Micromechanical RF-resonator

Ville Kaajakari<sup>1,2</sup>, Tomi Mattila<sup>1</sup>, Aarne Oja<sup>1</sup>, Jyrki Kiihamäki<sup>1</sup>, Hannu Kattelus<sup>1</sup>,  
Mika Koskenvuori<sup>2</sup>, Pekka Rantakari<sup>2</sup>, Ilkka Tittonen<sup>2</sup>, and Heikki Seppä<sup>1</sup>

<sup>1</sup>VTT Information Technology, P.O. BOX 1207, 02044 Espoo, Finland

<sup>2</sup>Helsinki University of Technology, Metrology Research Institute,  
P.O. BOX 3000, 02015 Espoo, Finland

## ABSTRACT

A micromechanical 13.1 MHz bulk acoustic mode (BAW) silicon resonator is demonstrated. The vibration mode can be characterized as a 2-D plate expansion that preserves the original square shape. The prototype resonator is fabricated of single-crystal silicon by reactive ion etching a silicon-on-insulator (SOI) wafer. The measured high quality factor ( $Q = 130000$ ) and current output ( $i_{MAX} \approx 160 \mu A$ ) make the resonator suitable for reference oscillator applications. An electrical equivalent circuit based on physical device parameters is derived and experimentally verified.

**Keywords:** RF-MEMS, resonator, SOI

## I. INTRODUCTION

Wireless data and sensing applications require high performance reference oscillators. Current state-of-the-art quartz crystal resonators are centimeter sized and consume milliwatts of power [1]. Micromechanical resonators offer a promise of low power consumption and integrability with IC electronics and are thus very attractive alternative for quartz in portable applications. Unfortunately, the efforts to demonstrate a micromechanical reference oscillator have suffered from the high electrical impedance and low power output of microresonators as demonstrated by our previously reported bulk acoustic wave (BAW) longitudinal mode beam resonator [2]. Although the BAW resonator demonstrated a high quality factor ( $Q = 180000$ ) compared to flexural resonators, the device was not able to provide adequate output signal level for a sufficiently low oscillator noise floor.

For a good reference oscillator, a resonator capable of both high quality factor and high power output is required. According to the Leeson's model for the phase noise, the near carrier noise is inversely proportional to the stored vibration energy and quality factor. The noise floor, however, is related to resonator signal power and is deteriorated with an increase in quality factor. Thus, a high quality factor alone is not enough for a good oscillator. To improve the overall oscillator phase noise performance, the resonator vibration energy has to be

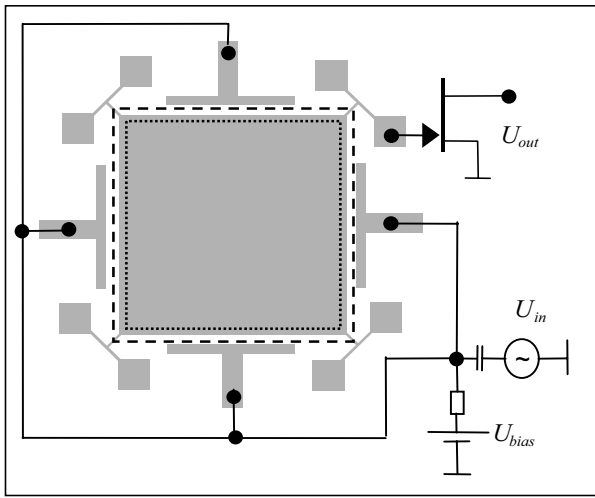
increased by increasing the vibration mass or amplitude. The upper limit for vibration amplitude is set by device nonlinearities [3]. This is different from quartz resonators that due to their large size can provide large signal amplitudes without being driven near the nonlinearity limit.

This paper describes a 13.1 MHz micromechanical resonator based on a 2-D extensional mode of a square plate with a quality factor of 130000 and high power handling capability. The device can be thought as an parallelization of 1-D beam resonators as it operates approximately at the same frequency as a longitudinal mode beam resonator with the same acoustic length. Compared to the 1-D resonator, the 2-D plate has approximately two orders-of-magnitude larger effective mass and electrode area leading to equivalent improvements in the motional resistance, maximum stored energy, and output current. Thus, the described resonator offers a crucial performance advantage which would for the first time provide phase noise typically required from quartz oscillators in wireless applications.

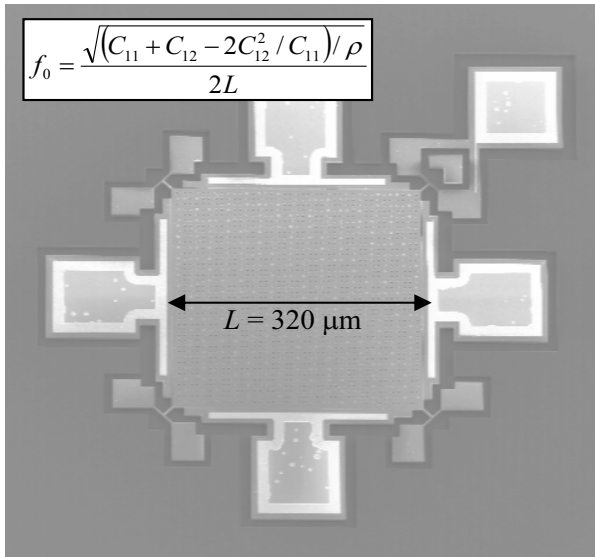
## II. RESONATOR STRUCTURE AND FABRICATION

Figure 1 shows a schematic and a scanning electron microscope (SEM) image of the resonator. As shown on the schematic, the vibration mode can be characterized as a square plate zooming in and out thus preserving the original shape. This is in contrast with the well-known Lamé-mode in which the square edges bend in antiphase preserving the plate volume [4]. Our resonator also exhibits the Lamé-mode (at  $f_0 = 12.1$  MHz,  $Q = 60000$ ), but using the symmetrical four-electrode configuration (Figure 1) it does not become excited.

The component was made by deep reactive ion etching of silicon-on-insulator (SOI) wafer. For HF release  $1.5 \mu m$  diameter holes were also etched into the plate. The resonator size was  $320 \mu m \times 320 \mu m \times 10 \mu m$ . The structural silicon layer was heavily boron doped ( $\rho_B \approx 5 \cdot 10^{18} \text{ cm}^{-3}$ ) for electrical conductivity. The surface orientation was (100) and the plate sides were aligned in [110] crystal directions. To keep the process flow simple, the electrical contact to the resonator was done with



(a) A schematic of the resonator showing the vibration mode and biasing and driving set-up. Dashed and dotted lines indicate expanded and contracted shapes.



(b) A scanning electron microscopic (SEM) image of the square-extensional resonator. Holes in the plate are for HF release etching.

**Figure 1.** Square-extensional microresonator ( $f_0 = 13.1$  MHz and  $Q = 130000$ )

corner anchoring so that the entire device could be fabricated with one mask. T-type corner anchoring was chosen to minimize energy leakage to the substrate. The one mask process also limited the minimum electrode gap width to approximately  $0.7 \mu\text{m}$ . Practical oscillators based on this resonator prototype may use more demanding processes to define smaller electrode gaps.

### III. RESONATOR MODEL

Figure 2 shows the square-extensional mode shape obtained with a finite element simulation. For an accurate analysis, a full 3-D model including the silicon

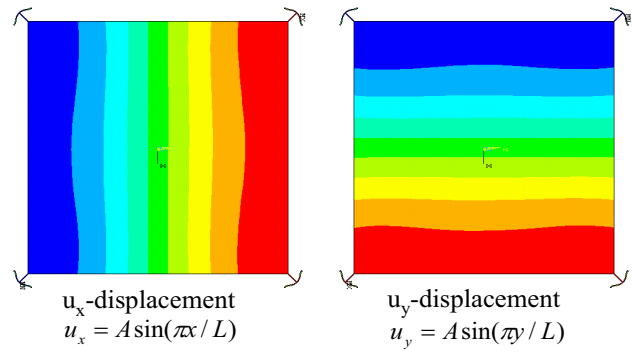


**Figure 2.** Mode shape obtained with 3D anisotropic FEM simulation. The square-extensional mode is a superposition of two sinusoidal waves. The plate retains the square shape in contrast with the Lamé-mode.

anisotropic elasticity was used. The mode can be approximated as a superposition of two orthogonal sound waves with displacements given by  $u_x = A \sin \pi x/L$  and  $u_y = A \sin \pi y/L$ , where  $A$  is the vibration amplitude and  $x$  and  $y$  indicate position on the plate. The square resonator shape, instead of circular, optimally accommodates the anisotropic elasticity of single-crystal silicon: the biaxial motion in  $x$ - and  $y$ -direction, with minimal rotation and shear, results from Poisson's ratio between  $[110]$ - and  $[\bar{1}10]$ -direction being very low ( $\nu = 0.06$ ). If the plate would have been oriented differently, for example in  $[100]$ -direction, the expansion mode would exhibit significant bending of the plate edges. This orientation dependency was verified with FEM simulations. By integrating the mode shape, a lumped one degree of freedom model valid near the resonance can be developed. Given that the mode shape is approximately two orthogonal sinusoids, the integration can be carried out explicitly leading to design equations suitable for “back of an envelope” calculations. The resulting equation of motion for the lumped vibration amplitude  $X$  is

$$m\ddot{X} + \gamma\dot{X} + kX = F(t), \quad (1)$$

where  $k$  is the effective spring constant,  $m$  is the effective mass,  $\gamma$  is the damping coefficient related to resonator quality factor by  $\gamma = \sqrt{km}/Q$ , and  $F(t)$  is the driving force [5]. The effective mass and spring constant can be related to the device geometry and are given by

$$\begin{aligned} m &= \rho h L^2 \\ k &= \pi^2 Y_{2D} h, \end{aligned} \quad (2)$$

where  $\rho$  is silicon density,  $h$  is device height, and  $Y_{2D}$  is the effective Young's modulus for the 2-D expansion. For a plate without holes this is  $Y_{2D} = C_{11} + C_{12} - 2C_{12}^2/C_{11} = 181$  GPa. The resonant frequency is then

$$f_0 = \frac{1}{2\pi} \sqrt{\frac{k}{m}} = \frac{1}{2L} \sqrt{\frac{Y_{2D}}{\rho}}. \quad (3)$$

The resonant frequency obtained with the lumped approximation and FEM simulation agree within 0.5% for a solid plate confirming the validity of the model. For a plate with etch holes, the resonant frequency is expected to be lower.

The capacitive driving force actuating the mass-spring system is

$$F(t) = U_{bias} \frac{\partial C}{\partial X} u_{ac}, \quad (4)$$

where

$$C = \epsilon_0 \frac{4L_{el}h}{d_0 + X} \quad (5)$$

is the transducer working capacitance that depends on electrode length  $L_{el}$  and nominal electrode gap  $d_0$ . Identifying the electromechanical coupling coefficient

$$\eta = U_{bias} \frac{\partial C}{\partial X} \approx -U_{bias} \frac{C_0}{d_0} \quad (6)$$

results in the relation between electrical current and mechanical transducer velocity

$$i = \eta \dot{X}. \quad (7)$$

Based on Equation (7), an electrical equivalent circuit shown in Figure 3 can be derived. The component values are

$$\begin{aligned} R_m &= \sqrt{km}/Q\eta^2 = k/\omega_0 Q\eta^2, \\ C_m &= \eta^2/k, \\ L_m &= m/\eta^2, \text{ and} \\ C_0 &= \epsilon_0 4L_{el}h/d_0. \end{aligned} \quad (8)$$

The equivalent circuit allows simulation of the resonator electrical response and provides design information on how scaling of the physical parameters affects the resonator performance. The first-order lumped model has also been refined to include effect of frequency shift due to bias voltage and capacitive and mechanical nonlinearity [3]. In the present study this model has been implemented with a circuit simulator program APlac and further information can be found in reference [6].

#### IV. MEASURED RESONATOR CHARACTERISTICS

The prototype resonator was measured with a HP4195A network spectrum analyzer. As the resonator impedance is rather high compared to the 50  $\Omega$  analyzer input/output impedance, a JFET (Phillips BF545B) preamplifier was used to provide an impedance conversion. Including the parasitics, the measured amplifier input impedance was approximately  $C_{in} = 6$  pF. The resonator was dc-biased with a 100 k $\Omega$  resistor. To minimize the shunt parasitic capacitance, the resonator substrate was grounded.

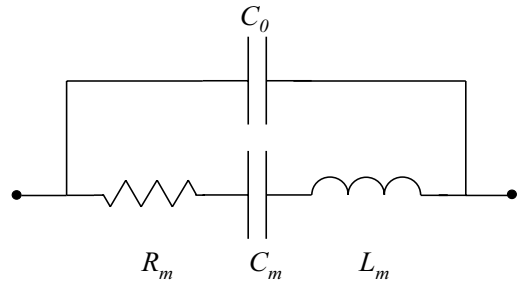


**Figure 3.** Electrical equivalent circuit for microresonator

**Table 1.** The resonator dimensions and characteristic parameters measured at  $U_{bias} = 100$  V.

Parameter	Symbol	Value	Units
Resonator side length	$L$	320	[ $\mu\text{m}$ ]
Electrode length	$L_{el}$	290	[ $\mu\text{m}$ ]
Resonator height	$h$	10	[ $\mu\text{m}$ ]
Transducer gap	$d_0$	0.75	[ $\mu\text{m}$ ]
Spring constant	$k$	16.2	[MN/m]
Effective mass	$m$	2.39	[nkg]
Quality factor	$Q$	130000	
Motional capacitance	$C_m$	20.8	[aF]
Motional inductance	$L_m$	7.07	[H]
Motional resistance	$R_m$	4.47	[k $\Omega$ ]

Figure 4 shows small signal level  $u_{ac} = 50$  mV transmission curves at different bias voltages showing good agreement with measured and simulated data. The mechanical resonance appears at  $f_0 = 13.112$  MHz, which is about 4.7% lower than estimated with FEM for a plate without etch holes. This corresponds to effective Young's modulus of 166 GPa. With increasing bias voltage, the resonator peak shifts to lower frequency due to capacitive spring effect. Based on the measured data, the mechanical unloaded quality factor is estimated to be  $Q = 130000$ . The other important resonator characteristics are summarized in Table 1.

In comparison with the previously reported 1-D beam [2], the square shape provides a much higher effective mass and electrode area while still maintaining the high quality factor of a silicon BAW device. The significantly lowered electrical impedance  $R_m = 4.47$  k $\Omega$  (vs.  $R_m = 1.05$  M $\Omega$  for the 1-D beam) makes noise matching to integrated electronics feasible. The maximum resonance current,  $i_{MAX} = 160$   $\mu\text{A}$  at the nonlinear limit, is more than two orders-of-magnitude larger than the current obtainable from the 1-D beam device. If operated at 10% of the hysteresis limit, the output current from the square-extensional mode resonator detected using a FET with input capacitance  $C_{in} = 1$  pF creates a signal voltage  $v_{in} = 194$  mV. Assuming fairly

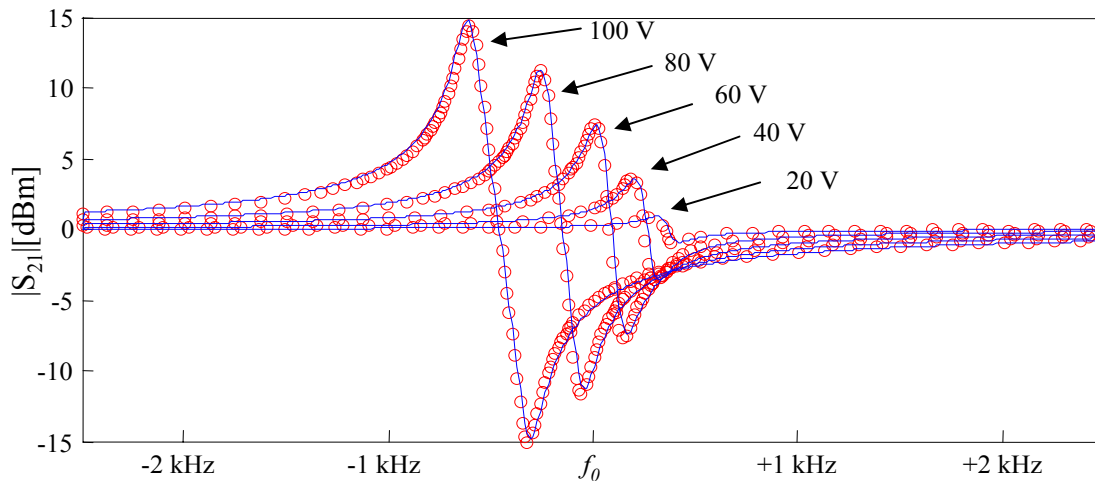


**Figure 4.** Measured ( $\circ$ ) and simulated ( $-$ ) transmission response ( $f_0 = 13.1$  MHz). Arrows indicate different bias voltages. Quality factor, gap spacing, and parasitic capacitance were adjusted for the best fit.

conservatively amplifier noise voltage of  $5 \text{ nV}/\sqrt{\text{Hz}}$ , this would allow a noise-floor below  $-155 \text{ dBc/Hz}$  in an oscillator application. Thus, reaching a noise floor of  $-150 \text{ dBc/Hz}$ , a typical GSM specification, appears feasible with integrated electronics. At this drive level, the energy dissipated in the resonator is  $1.1 \text{ }\mu\text{W}$  demonstrating low power consumption.

The rather high bias voltage used in the resonator measurements is a direct consequence of large  $0.75 \text{ }\mu\text{m}$  electrode gap used in the prototype. With an additional mask and fairly straightforward modification of the SOI fabrication process, it is possible to fabricate  $60 \text{ nm}$  gaps [7]. As the electromechanical coupling coefficient scales as  $\eta \sim U_{\text{bias}}/d_0^2$ , reducing the gap to  $100 \text{ nm}$  would allow effective impedance of  $64 \text{ }\Omega$  at  $15 \text{ V}$  bias voltage. Due narrowness of the gap, the capacitive nonlinearity dominates and the maximum vibration amplitude at the hysteresis limit is  $7.5 \text{ nm}$  [2]. The resonant current at 10% of the hysteresis limit is  $9.5 \text{ }\mu\text{A}$  leading noise floor of  $-150 \text{ dBc/Hz}$  with the same FET amplifier.

Finally, center anchoring of the resonator plate was studied by leaving an area approximately  $20 \text{ }\mu\text{m}$  square unreleased in the plate center. The devices with a solid center anchor had the same high quality factor proving that this anchoring method is viable. This is attractive as it reduces low, less than  $1 \text{ MHz}$ , resonances and improves the device shock resistance.

## V. CONCLUSIONS

This paper has demonstrated a bulk acoustic wave plate resonator operating at  $13.1 \text{ MHz}$  and having a quality factor of  $130000$ . The plate resonator offers nearly two orders-of-magnitude improvement both in motional resistance and output current in comparison to our prior work. Thus, the resonator shows for the first time that in

terms of phase noise RF-MEMS can be a viable alternative to macroscale quartz resonators.

## VI. ACKNOWLEDGMENTS

We thank V. Ermolov, H. Kuisma, and T. Ryhänen for useful discussions. The financial support from Nokia Research Center, VTI Technologies, and Finnish National Technology Agency is acknowledged.

## REFERENCES

- [1] E. Takahashi, O. Teshigawara, and K. Yamashita, "TCXOs Employing NS-GT Cut Quartz Crystal Resonators for Cellular Telephones", IEEE Int. Freq. Contr. Symp., 594 (1994).
- [2] T. Mattila et al., "12 MHz Micromechanical Bulk Acoustic Mode Oscillator", Sensors and Actuators A **101**, 1 (2002).
- [3] V. Kaajakari et al., "Nonlinearities in Single-Crystal Silicon Micromechanical Resonators", Transducers'03, (2003).
- [4] S. Basrou, H. Majjad, J.R. Coudevylle, and M. de Labacherie, "Design and Test of New High Q Microresonators Fabricated by UV-LIGA", SPIE Proc. **4408**, 310 (2001).
- [5] W. Weaver, Jr., S. Timoshenko, and D. Young, Vibration Problems in Engineering, 5th ed., (Wiley, 1990).
- [6] T. Veijola and T. Mattila, "Modeling of Nonlinear Micromechanical Resonators and Their Simulation with the Harmonic-Balance Method" Int. J. RF and Microwave Computer-Aided Eng. **11** 310 (2001).
- [7] E. Quévy, B. Legrand, D. Collard, and L. Buchailot, "Ultimate Technology for Micromachining of Nanometric Gap HF Micromechanical Resonators", MEMS'03, 157 (2003).